



**HAL**  
open science

## Validation of a Novel Sensing Approach for Continuous Pavement Monitoring Using Full-Scale APT Testing

Mario Manosalvas-Paredes, Kenji Aono, Shantanu Chakrabartty, Juliette Blanc, Davide Lo Presti, Karim Chatti, Nizar Lajnef

► **To cite this version:**

Mario Manosalvas-Paredes, Kenji Aono, Shantanu Chakrabartty, Juliette Blanc, Davide Lo Presti, et al.. Validation of a Novel Sensing Approach for Continuous Pavement Monitoring Using Full-Scale APT Testing. JOURNAL OF TRANSPORTATION ENGINEERING PART B-PAVEMENTS, 2023, 149 (1), 10.1061/jpeodx.0000397 . hal-04318028

**HAL Id: hal-04318028**

**<https://hal.science/hal-04318028v1>**

Submitted on 1 Dec 2023

**HAL** is a multi-disciplinary open access archive for the deposit and dissemination of scientific research documents, whether they are published or not. The documents may come from teaching and research institutions in France or abroad, or from public or private research centers.

L'archive ouverte pluridisciplinaire **HAL**, est destinée au dépôt et à la diffusion de documents scientifiques de niveau recherche, publiés ou non, émanant des établissements d'enseignement et de recherche français ou étrangers, des laboratoires publics ou privés.



Distributed under a Creative Commons Attribution - NonCommercial - NoDerivatives 4.0 International License



# Validation of a Novel Sensing Approach for Continuous Pavement Monitoring Using Full-Scale APT Testing

Mario Manosalvas-Paredes<sup>1</sup>; Kenji Aono<sup>2</sup>; Shantanu Chakrabarty<sup>3</sup>; Juliette Blanc<sup>4</sup>; Davide Lo Presti<sup>5</sup>; Karim Chatti, F.ASCE<sup>6</sup>; and Nizar Lajnef, Aff.M.ASCE<sup>7</sup>

**Abstract:** The objective of this paper is to present a novel approach for the continuous monitoring of pavement condition through the use of combined piezoelectric sensing and novel condition-based interpretation methods. The performance of the developed approach is validated for the detection of bottom-up fatigue cracking through full-scale accelerated pavement testing (APT). The innovative piezoelectric sensors are installed at the bottom of a thin 102 mm (4 in.) asphalt layer. The structure is then loaded until failure (up to 1 million loading cycles in this study). The condition-based approach, used in this work, does not rely on stain measurements and allows users to bypass the need for any structural or finite-element models. Instead, the data compression approach relies on variations in strain energy harvested by smart sensors to track changes in material and structural conditions. Falling weight deflectometer (FWD) measurements and visual inspections were used to validate the observations from the sensing system. The results in this paper present a first large-scale validation in pavement structures for a piezopowered sensing system combined with a new response-only based approach for data reduction and interpretation. The proposed data analysis method has demonstrated a very early detection capability compared to classical inspection methods, which unveils a huge potential for improved pavement monitoring. DOI: 10.1061/JPEODX.0000397. © 2022 American Society of Civil Engineers.

## Introduction

Flexible pavements are the most expensive assets in modern society (NAPA and EAPA 2011) and yet pavement engineers have not found a way to delay its weakening nor to provide an easy tool to monitor its condition (Ullidtz and Ertman Larsen 1989; Brown 1998; Xue et al. 2012; Robbins et al. 2017). Pavements, as any other structure, age and deteriorate as a function of time; these effects are accelerated by asphalt mixture aging (Xue et al. 2014), cumulative loading (Brown and Peattie 1974; Dessouky et al. 2014), environmental conditions (Leiva-Villacorta et al. 2016), and/or inadequate maintenance. Thus, knowing its current condition and estimating

its future performance is a matter of high importance for road owners and decision makers (Lajnef et al. 2013). New developments for evaluating pavement condition using in situ pavement sensors (Sohn et al. 2003; Lajnef et al. 2011; Manosalvas-Paredes et al. 2019; Bahrani et al. 2020; Iodice et al. 2021) are an alternative to the more traditional destructive methods and external evaluation methods (Verma et al. 2013; Marecos et al. 2017). Detecting damage at its earliest stages is important for almost every industry. Farrar and Worden (2007) defined damage as the change of material and/or geometrical properties of the system including changes of the boundary conditions and system connectivity. It is worth mentioning that most damage detection methods rely on comparing the mechanical response of the damaged structure, which most of the time come from computer simulations, to the intact state or undamaged state (Del Grosso 2013). In addition, damage does not necessarily imply a total loss of system functionality but rather that the system is no longer operating in its optimal manner. Thus, damage grows until it reaches a point in which it affects the system operation and is no longer acceptable to the user (Sohn et al. 2003; Brownjohn 2007).

The previous definitions tie perfectly with what pavements engineers have been using to define damage over the last decades in terms of structural capacity (layer moduli) (Manosalvas-Paredes et al. 2017) or functional performance [international roughness index (IRI), present condition index (PCI)] (Susanna et al. 2017). Outlining thresholds for assessing pavement condition is not a simple task; therefore, continuous monitoring is foreseen as a solution for the coming years (Alavi et al. 2016). So far, neither functional nor structural evaluation has fulfilled, by itself, those requirements and has opened the door for new technologies to arise such as structural health monitoring (SHM) (Sohn et al. 2003; Brownjohn 2007; Farrar and Worden 2007). The most widely accepted definition for SHM refers to the process of implementing a damage identification strategy for aerospace, civil, and mechanical engineering infrastructure (Farrar and Worden 2007; Di Graziano et al. 2020). SHM ought to provide the tools to progress from common, but erroneous, time-based maintenance philosophies to a more cost-effective condition-based maintenance philosophy. Nonetheless, technical

<sup>1</sup>Ph.D. Researcher, Nottingham Transportation Engineering Centre, School of Civil Engineering, Univ. of Nottingham, University Park, Nottingham NG7 2RD, UK (corresponding author). ORCID: <https://orcid.org/0000-0002-7068-6365>. Email: [mario.manosalvas@ptsinternational.co.uk](mailto:mario.manosalvas@ptsinternational.co.uk)

<sup>2</sup>Postdoctoral Research Associate, Dept. of Computer Science and Engineering, Washington Univ. in St. Louis, St. Louis, MO 63130. ORCID: <https://orcid.org/0000-0002-7192-0061>

<sup>3</sup>Professor, Dept. of Computer Science and Engineering, Washington Univ. in St. Louis, St. Louis, MO 63130.

<sup>4</sup>Principal Researcher, Materials & Structures Department—Laboratoire Auscultation, modélisation et expérimentation sur les infrastructures de transports, Univ. Gustave Eiffel, Institut Français des Sciences et Techniques de l'Aménagement et des Réseaux, Campus de Nantes, Bouguenais F-44344, France.

<sup>5</sup>Assistant Professor, Dept. of Engineering, Univ. of Palermo, Ed 8, Palermo 90128, Italy.

<sup>6</sup>Professor, Dept. of Civil and Environmental Engineering, Michigan State Univ., East Lansing, MI 48824. ORCID: <https://orcid.org/0000-0002-7749-7583>

<sup>7</sup>Associate Professor, Dept. of Civil and Environmental Engineering, Michigan State Univ., East Lansing, MI 48824.

Note. This manuscript was submitted on May 5, 2021; approved on May 11, 2022; published online on October 27, 2022. Discussion period open until March 27, 2023; separate discussions must be submitted for individual papers. This paper is part of the *Journal of Transportation Engineering, Part B: Pavements*, © ASCE, ISSN 2573-5438.

challenges have been identified (Doebbling et al. 1996; Sohn et al. 2003) and will have to be addressed before a true implementation occurs. Therefore, this paper investigates the operational evaluation and data acquisition, normalization, and data reduction of a novel self-powered sensor developed at Michigan State University (MSU) (Alavi et al. 2016; Hasni et al. 2017) and compares it with two commercial strain gauges from well-known manufacturers, Dynatest and Tokyo Measuring Instruments Laboratory. Advantages of the piezo-powered sensing system compared to conventional strain gauges include: low power requirements (80 nW), self-powered continuous sensing, low cost, small size, autonomous computation and nonvolatile storage of sensing variables, and wireless communication (Lajnef et al. 2013).

The objective is to validate the compressed cumulative loading event approach, implemented in the previously developed piezofloating-gate (PFG) sensor (Chatti et al. 2016), in detecting bottom-up fatigue cracking through full-scale testing at The French Institute of Science and Technology for Transport, Spatial Planning, Development and Networks (IFSTTAR) circular test track by measuring longitudinal strains at the bottom of the asphalt concrete (AC). Falling weight deflectometer (FWD) measurements were performed at 0.0, 0.5, and 1.0 million loads and were used as reference points. Layered elastic theory (LET) was used for back-calculating the layer moduli for the different layers and for obtaining the pavement responses at different depths using the French standard axle of 13 t composed of dual wheels (Corté and Goux 1996).

This paper is structured as follows. A description on the piezoelectric sensor and the implementation “Data Compression Protocol” are first introduced. After that the paper concentrates on “Accelerated Pavement Test Setup” and “Methodology” where the test sections, sensors distribution, basic technologies, and the experimental measurements. “Results” and “Discussion” sections where FWD measurements and sensors data results are presented. Finally, the “Conclusion” of this paper are as well as recommendations for further research are outlined.

## Piezoelectric Sensors and Data Compression Protocol

Piezoelectric sensors have become more popular in strain and vibration sensing due to their ability to harvest mechanical energy from ambient variations. In that sense, researchers at Michigan State University have shown that piezoelectric transducers, under traffic loading, can harvest the induced microstrain deformation in the asphalt layer to power up the electronics of the novel PFG sensor (Lajnef et al. 2011; Chatti et al. 2016; Hasni et al. 2017).

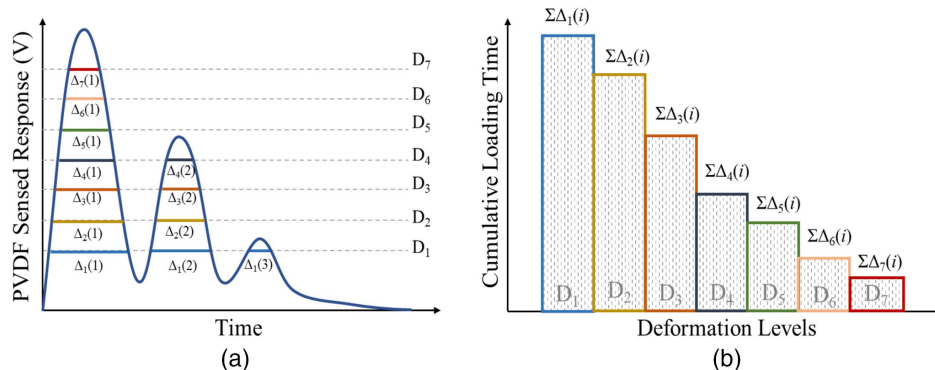


Fig. 1. (a) PVDF work representation; and (b) clustered histogram. (Data from Lajnef et al. 2013.)

A complete description of the sensor can be found in Lajnef et al. (2013), Aono (2017), Aono and Pochettino (2018), and Aono et al. (2019).

Within this research, a rectangular polyvinylidene fluoride (PVDF) membrane, similar to the one installed in the PFG sensor, was used to sense the deformations. Fig. 1(a) shows a general representation on how the PVDF measures whereas Fig. 1(b) shows how the measurements are clustered in a histogram, which can be represented as a cumulative distribution function (CDF), Eq. (1). Statistical parameters of the CDF such as the mean ( $\mu$ ) and the standard distribution ( $\sigma$ ) can be considered as indicators of damage progression whereas  $\alpha$  and  $g$  are fitting constants (Hasni et al. 2018)

$$F(\varepsilon) = \frac{\alpha}{2} \left[ 1 - \operatorname{erf} \left( \frac{(g - \mu)}{\sigma\sqrt{2}} \right) \right] \quad (1)$$

The novelty behind the proposed data compression protocol is that all external parameters affecting the change in pavement responses (i.e., traffic loads, environment, construction, and so on) can be grouped within the distribution of measurements over time. Thus, the only parameter able to cause a *shift* in the CDF is the formation of damage in the structure represented by the number of threshold levels ( $D_1$  to  $D_7$ ) that are open.

## Accelerated Pavement Test Setup

This section presents an overview of the elements that are needed to perform an accelerated pavement test (APT).

### Circular Test Track

The circular test track (CTT), Fig. 2, developed by IFSTTAR, is an outdoor APT dedicated to full-scale pavement experiments. The CTT has a central electrohydraulic motor unit which can be equipped with various load configurations simulating half-axles of heavy vehicles (Nguyen et al. 2013). The CTT has a track average perimeter of 120 m and can be loaded at a maximum speed of 100 km/h.

### Sensors Outline

Fig. 3 shows the distribution of both traditional and piezoelectric sensors placed at the bottom of the asphalt layer. As it is seen, a majority of the sensors were placed parallel to the direction of the load; Sensor H4 is the only one placed perpendicular to the direction of the load. Finally, Sensors H5, H6, and H8 were placed at radii of 18.40, 18.70, and 19.30 m, respectively, to study the effect of varying the position of the load wandering during testing.



Fig. 2. IFSTTAR circular test track.

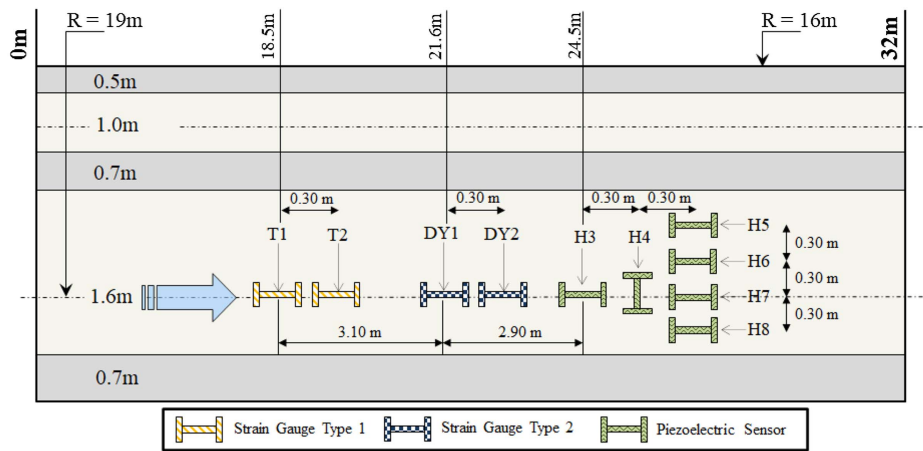


Fig. 3. Sensors outline along the circular test track, not to scale.

### Traditional Instrumentation

A brief description of the two commercial strain gauges follows.

#### Tokyo Measuring Instruments Lab

Strain gauge type KM-100HAS (Tokyo Measuring Instruments Lab, Tokyo, Japan) has an apparent elastic modulus of approximately  $40 \text{ N/mm}^2$ , resistance of  $350\text{-}\Omega$  full bridge, rated output approximately of  $2.5 \text{ mV/V}$ , capacity of  $\pm 5,000 \times 10^{-6}$  strain, and temperature range between  $-20^\circ\text{C}$  and  $180^\circ\text{C}$ .

#### Dynatest PAST-II-AC

The Dynatest PAST-II-AC (Dynatest, Ballerup, Denmark) is an H-shaped precision transducer specially manufactured for strain measurements in hot-mix asphalts. The transducer has an apparent elastic modulus of approximately  $2.2 \text{ N/mm}^2$ , a resistance of  $120\text{-}\Omega$  quarter bridge, physical range of up to  $1,500 \mu\epsilon$ , sensitivity of  $0.11 \text{ N}/\mu\epsilon$ , and temperature range between  $-30^\circ\text{C}$  and  $150^\circ\text{C}$ .

### Materials

Table 1 shows the mechanical properties of the coarse aggregate (NEN 2020; EN 2012, 2020a, b) used to manufacture the high modulus asphalt mix [enrobé à module élevé (EME)] EME2, which is a high-performance asphalt mix used for base layers. EME2 is

Table 1. Characteristics of the aggregates according to the European Union specification system

Test and standard	Requirement	Fraction 10/14 mm
Percentage of crushed surfaces, % of mass (EN 933-5)	100	100
Flakiness index (EN 933-3)	$\leq 20$	07
Los Angeles abrasion (EN 1097-2)	$\leq 15$	09
Polished stone value (EN 1097-8)	$\geq 56$	$> 50$

made out of 20% reclaimed asphalt and a hard binder of 20/30 penetration grade, with a total binder content of 5.5%. EME2 asphalt mixtures are commonly used in France for base layers, and it is considered a reference material with a well-known behavior. Pavement structure is composed of three layers: 102 mm of asphalt, 760 mm of unbound granular base, and 1,600 mm of stone bed as subgrade, see Fig. 4.

### Methodology

The APT started on November 14, 2017, and finished on February 15, 2018, and a total of 999,200 load repetitions were applied. Each arm (four in total) was equipped with a single-axle dual-wheels and carried 65 kN corresponding to half of the standard French axle



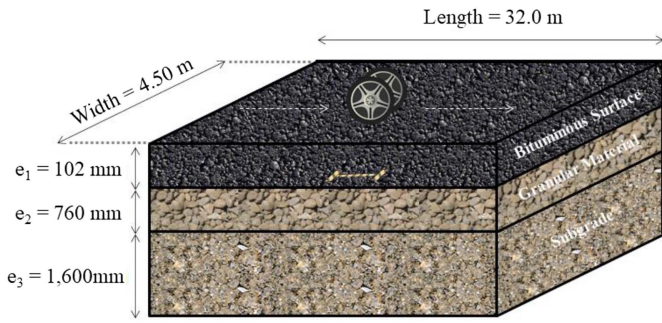


Fig. 4. Representation of the pavement structure.

load (Corté and Goux 1996). An approximate velocity of 76 km/h corresponding to 10.0 rounds per minute was used to move the arms around the CTT. During the APT, FWD measurements, visual observation, and sensor measurements were made at different time steps to monitor its evolution. These are described hereafter.

### FWD Measurements

Measurements were made at 0.0, 0.5, and 1.0 million load repetitions with a Dynatest FWD model 8002-077. Deflections were used to back-calculate the individual layer moduli of the pavement based on the layered elastic theory. Results were used as control points.

### Visual Observation

The extent of cracking is defined as percentage of cracked length, Eq. (2), where  $L_i$  represents the length of cracked zone. For

longitudinal cracks, the crack length corresponds to the measured length of the cracks whereas for transverse cracks, a length of 500 mm is conventionally attributed to each crack. Surface cracks were marked with different colored paints in order to identify their evolution in time

$$\text{Extent of cracking(\%)} = \frac{\sum_i L_i}{L} \quad (2)$$

### Sensor Measurement

Sensor measurements from strain gauges and piezoelectric sensors were made at approximately every 20,000 loads. Nonetheless, in order to determine which sensors survived construction, a first batch of measurements was collected after only 5,000 loads.

Fig. 5(a) shows the strain pulse time histories after 5,000 loads for commercial Strain gauges L1, L2, and DY2. Fig. 5(b) shows the first four strain pulses, grouped, for strain gauge DY2 as well as the mean pulse considered as representative and illustrated by a continuous line. Similarly, piezoelectric measurements in terms of voltage were also recorded at 5,000 loads. Fig. 6(a) shows the measured voltage for Sensor H3 and Fig. 6(b) shows the mean voltage where some noise is seen. The shape of the voltage signal is different from the strain signal shape for two reasons: (1) the selected piezotransducers for this work were designed to respond only to tension and not in compression; and (2) the negative voltage component is generated during the unloading phase. The overall signal is thus descriptive of the tensile loading and unloading phases, the critical components for fatigue damage.

The maximum peak values from the strain gauges and piezoelectric sensors are then used to track pavement response and damage evolution with increasing number of load repetitions.

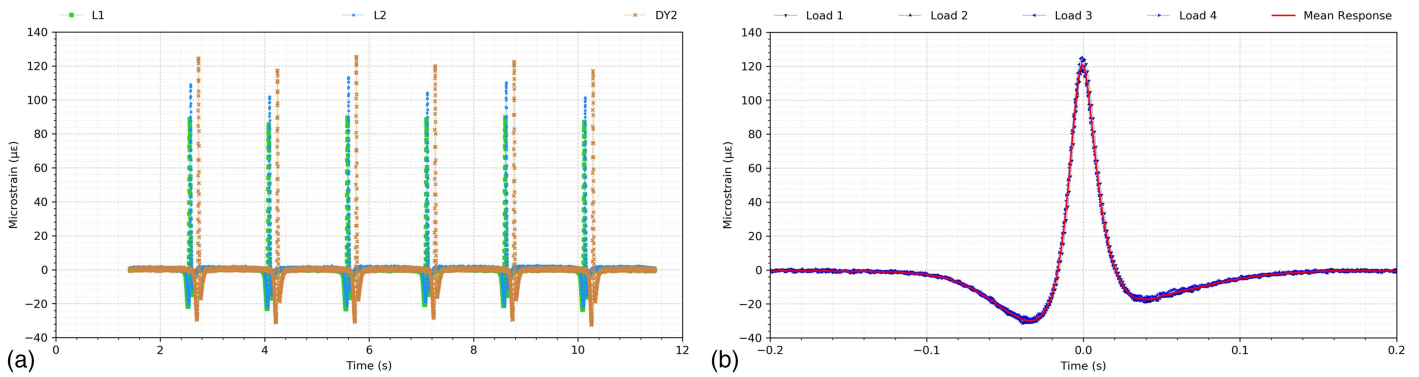


Fig. 5. (a) L1, L2, and DY2 strain pulse; and (b) DY2 mean pulse.

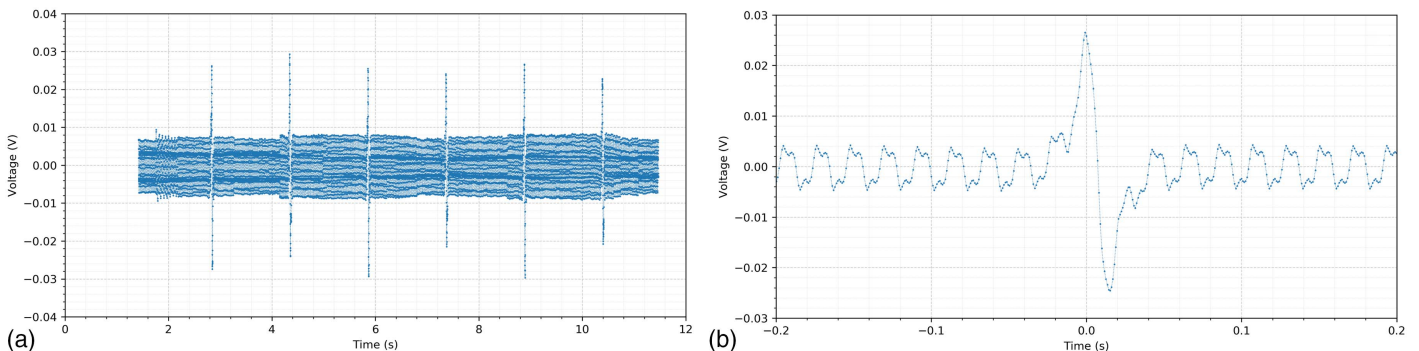


Fig. 6. (a) H3 sensor voltage; and (b) H3 mean voltage.

## Experimental Results

This section presents the results and interpretation of the measured data.

### FWD Measurements

Deflections are the most used parameter by pavement engineers to relate the structural condition of a pavement. Center deflection is associated with the overall state of the pavement while the deflection basin, generated by the outer geophones, is associated with the condition of the underlying layers.

### Deflection Data

Figs. 7–9 show the change in deflection profiles in which it is seen how the variability in measurement increase with the number of load repetitions. Higher variations occur between the center deflection and deflections measured at 600 mm from the center, allowing the researchers to believe that the majority of damage occur in the upper layers.

Fig. 10 corroborates the previous statement as it shows the change in deflection, absolute value, between 0.5 and 1.0 million loads. Comparison has been made at Stations 7, 12, 18, 24, and 29 m. In here, it is seen that the major changes occur between 18 and 29 m, where deflections increase to around 120 microns and that the majority of change is limited to the upper layers.

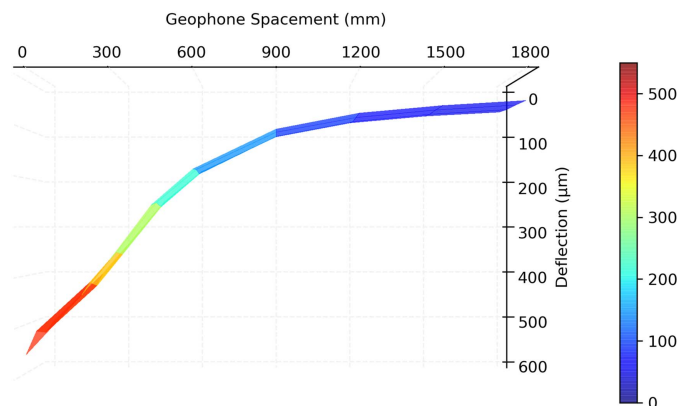


Fig. 7. Deflection profile at 0.0 million load repetitions.

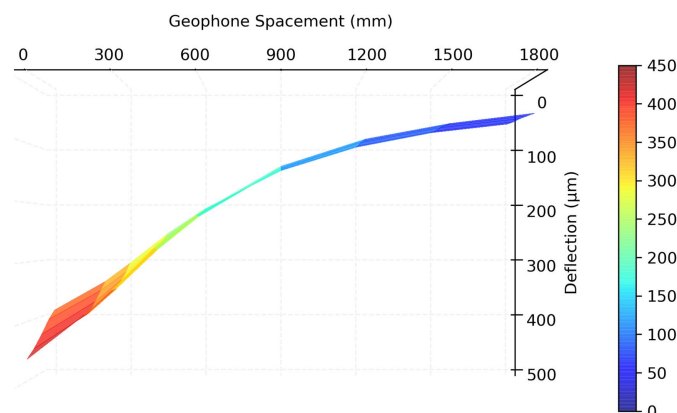


Fig. 8. Deflection profile at 0.5 million load repetitions.

### Layer Moduli Back-Calculation

Back-calculation is a mechanistic evaluation of pavement structural response that uses the deflections measured and attempts to match them with the calculated deflections by adjusting the pavement layers moduli. Back-calculation is an iterative procedure in which the layer thickness is a key input. This research has used Dynatest ELMOD version 6 software to back-calculate the different layer moduli of the pavement. Moreover, this research has limited the thickness of the unbound granular base to 350 mm for the analysis. Fig. 11 show the back-calculation process in which the measured and calculated deflections are compared. Absolute differences in deflections have been chosen for the acceptance criteria. Table 2 shows the average moduli and standard deviation (STDV) for the different layers at 0.0, 0.5, and 1.0 million loads. Back-calculated asphalt moduli has been corrected to a reference temperature of 20°C following Highways England CS 229 “Data for Pavement Assessment” Equation 4.45 (DMRB 2020).

### Pavement Responses

Theoretical pavement responses have been calculated using a dual-wheel single-axle configuration to carry the 13-t load, tire pressure of 0.66 MPa, and wheel distance (center to center) of 376 mm. Table 3 shows the horizontal tensile strain at the bottom of the asphalt layer (102 mm) and the vertical compressive strain on the surface of the subgrade (452 mm) at 0.0, 0.5, and 1.0 million loads, respectively. Finally, the relative standard deviation (RSD) is included to show the variability of the results with time (damage).

### Visual Observation

Fatigue performance was evaluated visually by recording the cracks on the pavement surface as a function of the number of applied loads. The first surface cracks appeared after 0.9 million load repetitions and were represented with a white line, see Fig. 12. At the end, a total cracked area of 4.0% was reported.

### Sensors Measurements

Fig. 13 shows the evolution of average sensor responses with number of load repetitions. Fig. 13(a) show responses for commercial Strain gauge DY2 in which it is seen how the maximum longitudinal strain increases from 121 to 194  $\mu\epsilon$  and finally to 276  $\mu\epsilon$ . Fig. 13(b) on the other hand show responses for piezoelectric Sensor H3 in which it is seen how the measured voltage goes from 0.027 to 0.026 V and finally to 0.059 V. Voltage measurements

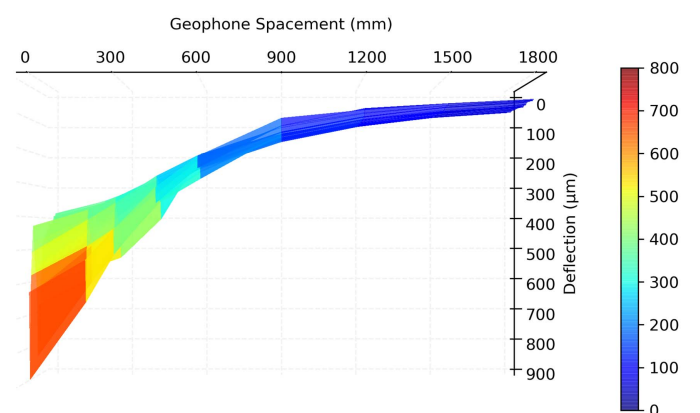


Fig. 9. Deflection profile at 1.0 million load repetitions.

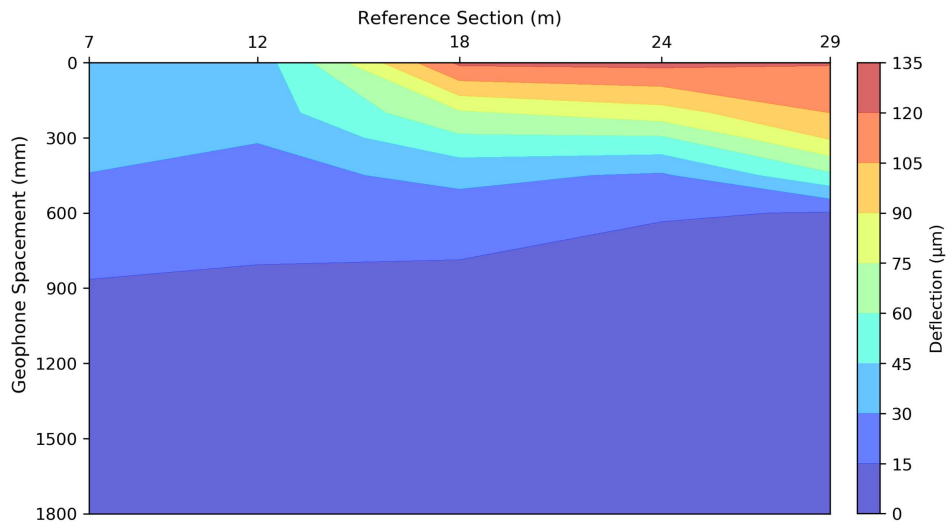


Fig. 10. Change in deflections absolute value between 0.5 and 1.0 million load repetitions.

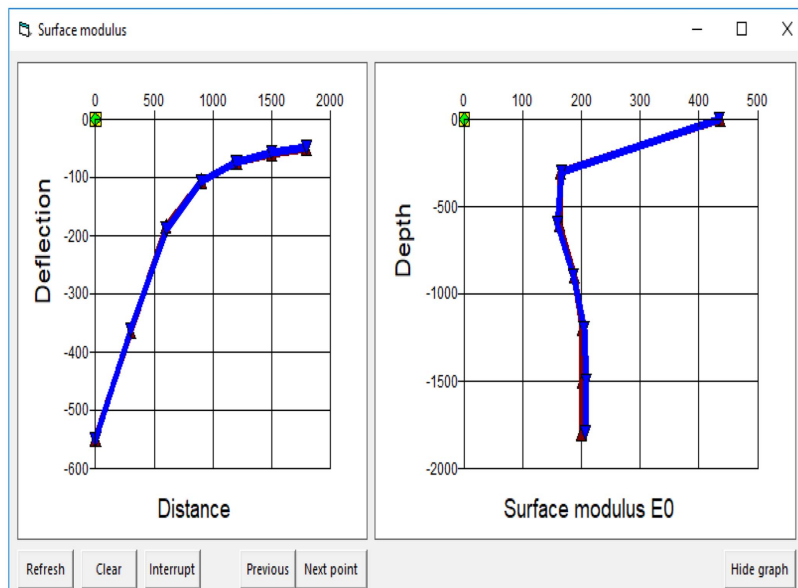
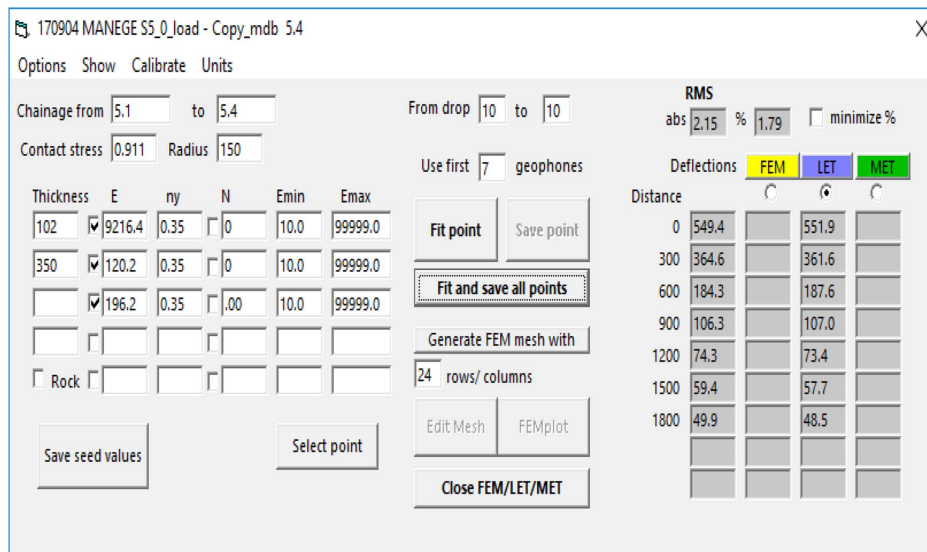


Fig. 11. Back-calculation following LET at 0.0 million load repetitions.



**Table 2.** Back-calculation average values at 0.0, 0.5, and 1.0 million load repetitions

Load (millions)	T (°C)	Layer						
		AC (MPa)	AC 20°C (MPa)	STDV	UGM (MPa)	STDV	Subgrade (MPa)	STDV
0	27.9	10,524	16,395	1.08	122	1.04	202	1.03
0.5	10.3	27,529	17,973	1.16	115	1.09	167	1.03
1	12.6	18,423	13,152	1.91	98	1.28	158	1.08

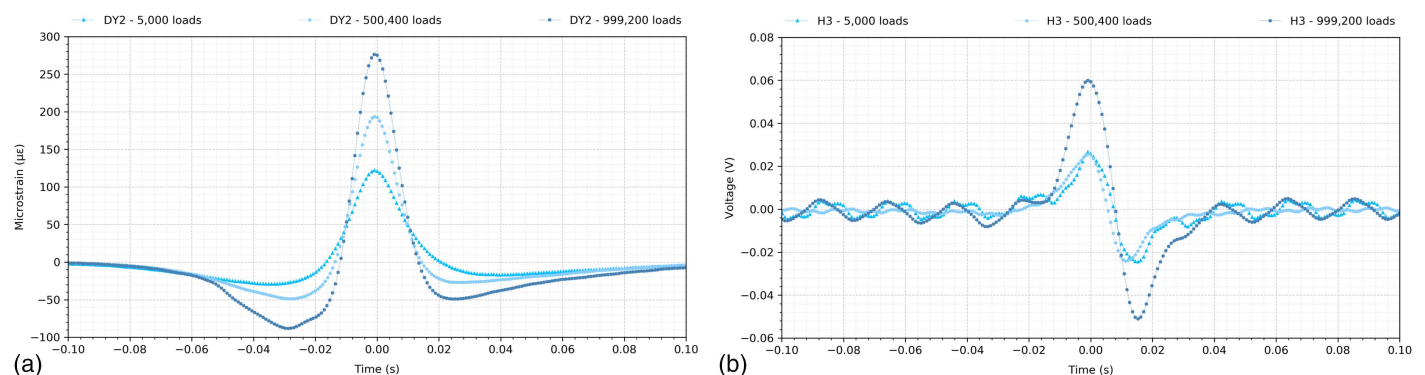
**Table 3.** Average pavement responses at 0.0, 0.5, and 1.0 million load repetitions

Load (millions)	Horizontal tensile strain			Vertical compressive strain		
	Average	STD	RSD (%)	Average	STD	RSD (%)
0.0	-116.13	6.8	-5.9	212.93	9.2	4.3
0.5	-125.90	13.8	-10.9	252.95	20.7	8.2
1.0	-211.75	106.14	-50.1	306.30	85.94	28.1

**Fig. 12.** Condition of the pavement after 1.0 million load repetitions.

remain nearly the same for the first half of the test followed by a rapid growth.

Fig. 14 shows the increment of the average maximum longitudinal strain (DY2) and sensor voltage (H3) throughout the entire test. As it is seen, both trends correspond to each other, especially after about 600,000 load repetitions when the responses increase.

**Fig. 13.** Evolution of sensor responses with number of load repetitions.

Figs. 15 and 16 show the novel sensing approach called cumulative voltage time (CVT) for piezoelectric Sensors H3 and H7, respectively. The CVT is calculated when the input signal (voltage) exceeds one or more of the preset threshold levels, after which, the integrated voltage-time value is recorded (Alavi et al. 2016). The resulting value is proportional to the strain above the selected threshold level, and it is referenced to in this paper as a threshold level, see Fig. 1.

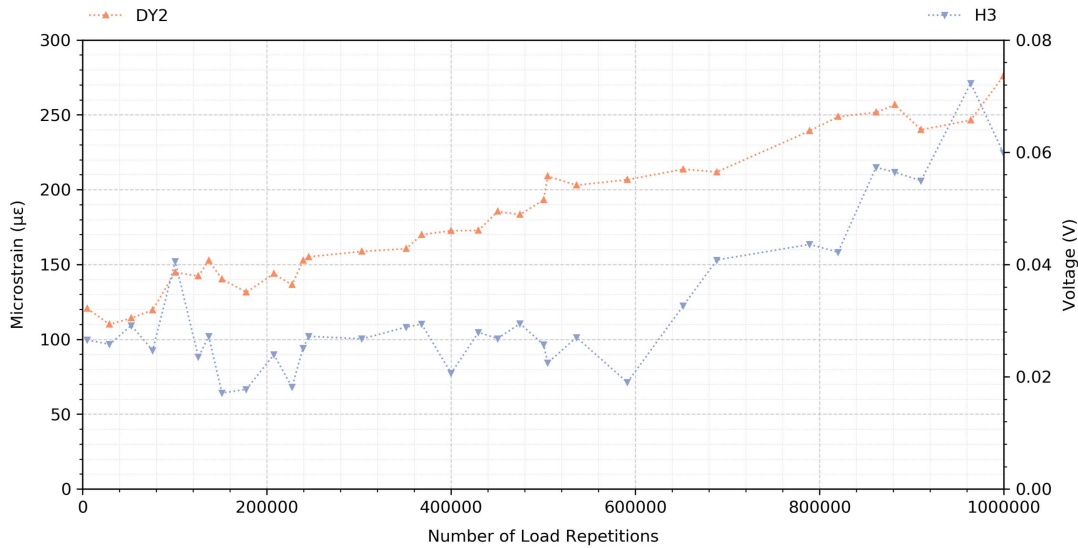
Fig. 15 shows that the rate of increase in CVT for piezoelectric Sensor H3 (longitudinal sensor voltage) increases after about 600,000 load repetitions, which is linked to the waking-up of higher thresholds (Levels 4 and 5). The same behavior is seen after about 800,000 load repetitions in which the highest thresholds (Levels 6 and 7) wake up. Fig. 16 does not show a clear increase in rate for the higher threshold values (Levels 4 and higher); however, it shows a mild increase after about 400,000 cycles, suggesting an appearance of damage initiation.

## Discussion

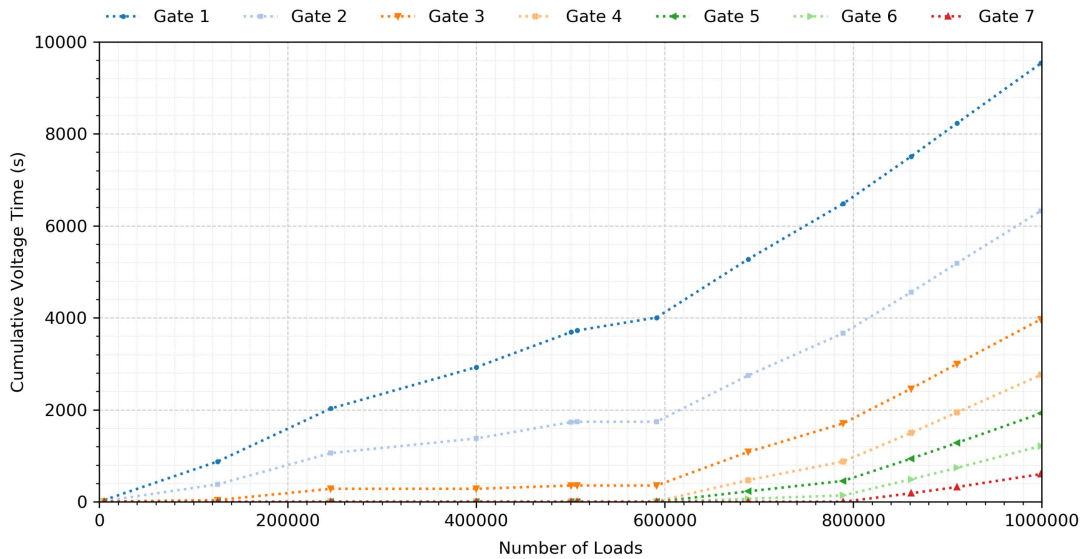
Deflection profiles, see Fig. 10, have shown that the higher variation in deflections occurred between 18 and 24 m of the test section. Fig. 17, on the other hand, summarizes these variations in percentage considering the entire deflection basin between 0.5 million loads, see Fig. 8, and 1.0 million loads, see Fig. 9, repetitions. Once again it is seen that the main differences occurred in the upper layers (from  $G_1$  to  $G_3$ ), whereas the outer geophones ( $G_6$  and beyond) show relatively lower changes. Based on this, it can be concluded that most of the damage is taking place in the asphalt layer.

Fig. 18 shows the theoretical reduction in the asphalt layer modulus with the increase in load repetitions, between 0.5 and 1.0 million load repetitions. This research has found a reduction in the asphalt moduli of 3%, 52%, 49%, and 32% for Stations 12, 18, 24, and 29 m, respectively. Reductions of 50% or more in the asphalt concrete modulus is considered as a failure criterion





**Fig. 14.** Longitudinal strain and sensor voltage evolution throughout the entire test (DY2 data in microstrain and H3 data in voltage).



**Fig. 15.** Sensing approach responses from Sensor H3 versus number of loads.

(Manosalvas-Paredes et al. 2017). This research found the lowest asphalt modulus, after 1.0 million load repetitions, at Station 22 m with a value of 4,361 MPa.

This research focuses on pavement responses; hence, Fig. 19 shows the theoretical changes in calculated strains using the back-calculated moduli. For Stations 12, 18, 24, and 29 m, the increment in the longitudinal strain, between 0.5 and 1.0 million load repetitions, is 5%, 95%, 70%, and 99%, respectively. Furthermore, Figs. 18 and 19 show a clear inverse relation between their responses (decrease in modulus results versus an increase of the strain). These results confirm what was presented in Fig. 10, showing that the critically damaged area is located between Stations 18 and 29 m.

Visual observations are clearly not a good approach for detecting early pavement deterioration because it may be too late when cracks appear at the surface of the pavement (for classical bottom-up fatigue). In this experiment, the first surface cracks were

observed shortly after 900,000 load repetitions; on the other hand, piezoelectric sensors with the novel data approach showed an increase in responses just after 600,000 load repetitions, thus warning the user of possible surface cracks in the near future so it could be avoided or delayed through proper maintenance activities. This behavior is seen in Fig. 15 (H3 longitudinal sensor voltage) in which the CVT starts activating (change in trend) more levels after 600,000 load repetitions indicating that damage is starting to occur. Highest levels (Threshold 6 and 7) are only activated after 900,000 load repetitions, which relates perfectly with the visual observation. Fig. 16 on the other hand shows a weaker increase in trend, indicating that the appearance of surface cracks will take a longer time to materialize, suggesting that fatigue cracking was better assessed using piezoelectric Sensor H3.

When the strain amplitude starts to increase under the repetitive loading, the harvested voltage increases as well, which resulted in activating higher threshold levels. Finally, it is seen that the

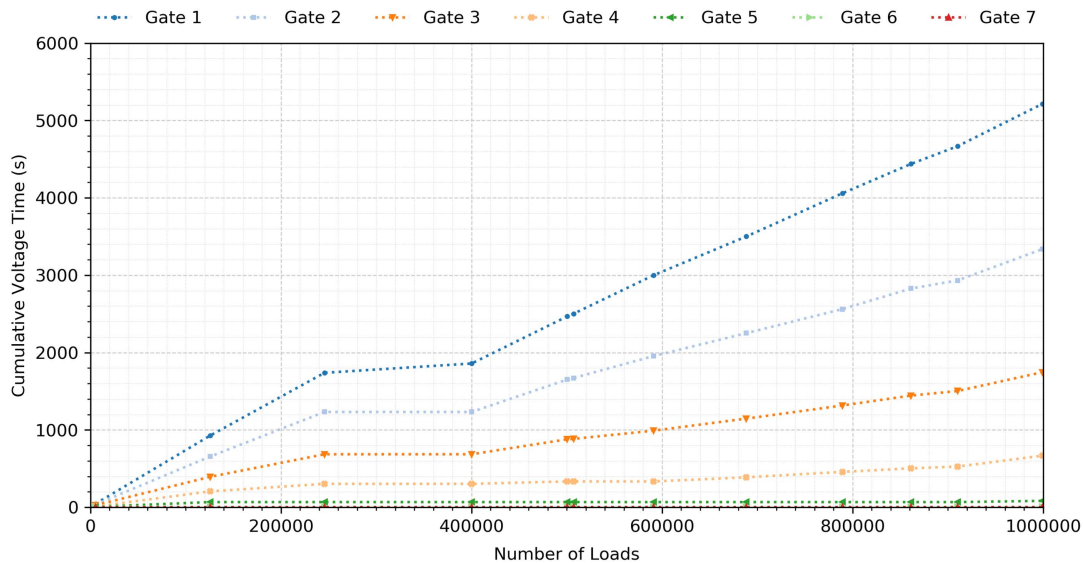


Fig. 16. Sensing approach responses from Sensor H7 versus number of loads.

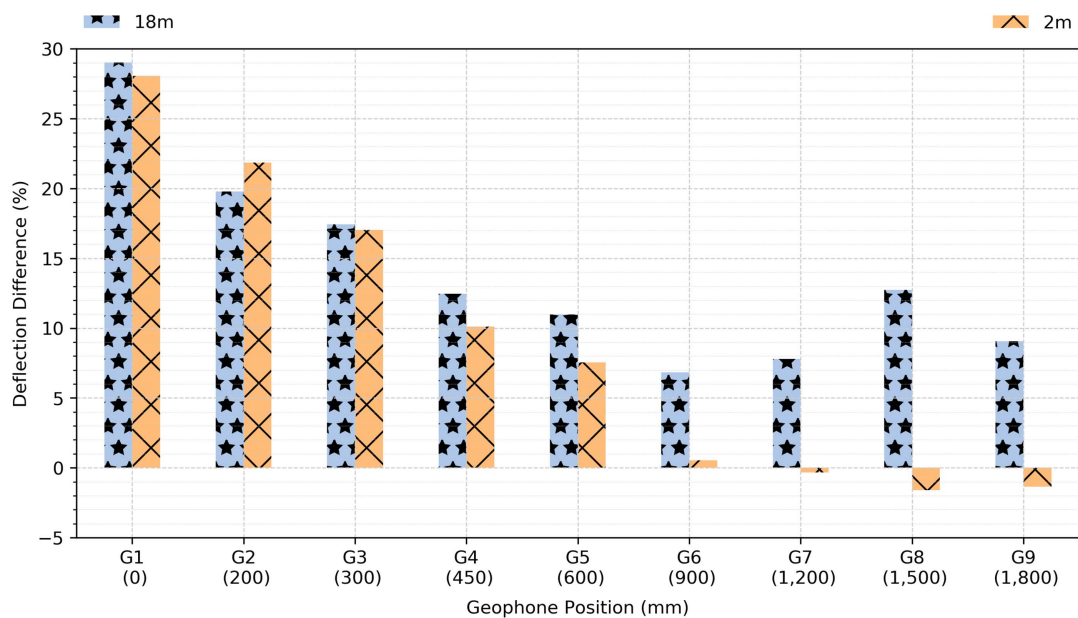


Fig. 17. Deflection changes from 0.5 to 1.0 million load repetitions.

threshold level activation is a good indicator of damage severity. Higher levels are sensitive to high strains (i.e., to severe cracking) whereas lower levels are useful to detect the early onset of fatigue cracking.

## Conclusions

This paper presented, for the first time, an approach for monitoring pavement condition based on piezoelectric sensors technology through a full-scale accelerated pavement testing experiment. The novel idea in this research is to use the cumulative strain statistics experienced by the pavement structure instead of the entire time-history. This will benefit self-powered sensors by reducing the amount of data to transmit wirelessly and optimize the energy consumption of the whole system.

From the results and discussion presented, in which pavement deterioration increased with increasing number of load repetitions, it is concluded that the new type of piezoelectric sensor has been successfully validated with a worldwide known strain gauge in full-scale testing environment.

This research has found that the cumulative loading time of piezovoltage is a good indicator of damage progression and the timing of the activation of sensor thresholds with different voltage levels are good indicators of damage severity. This finding is significant given that the results are from sensors that have been installed in a full-scale pavement section that has been subjected to fatigue testing, thus confirming the validity of the sensors early detection of fatigue damage outside laboratory conditions.

The results of this phase validated the potential of using self-powered piezofloating-gate sensors for fatigue assessment of pavements under real operating conditions. Thus, the next research

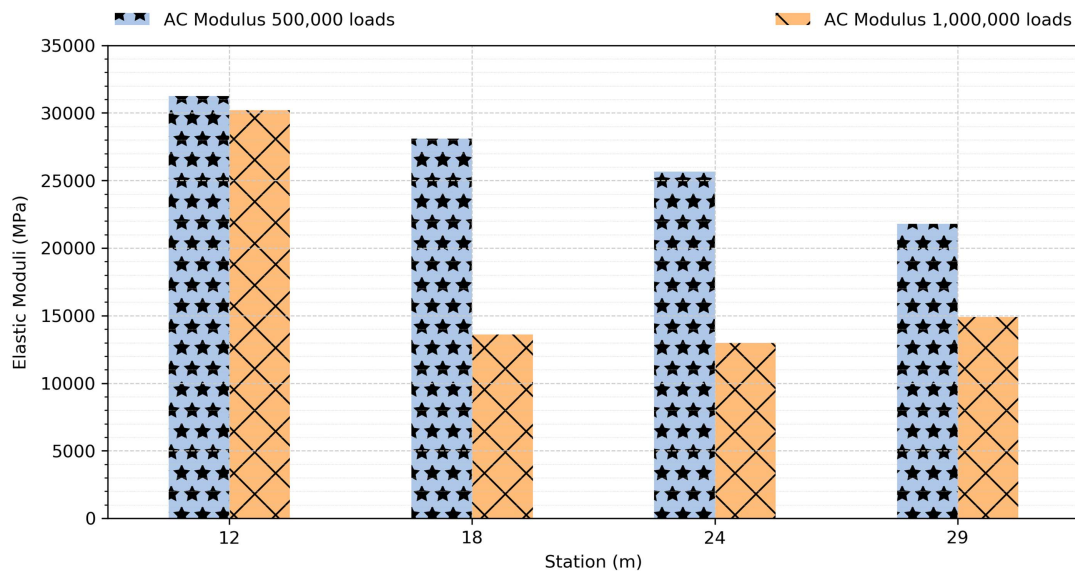


Fig. 18. Difference in back-calculated asphalt moduli for different stations.

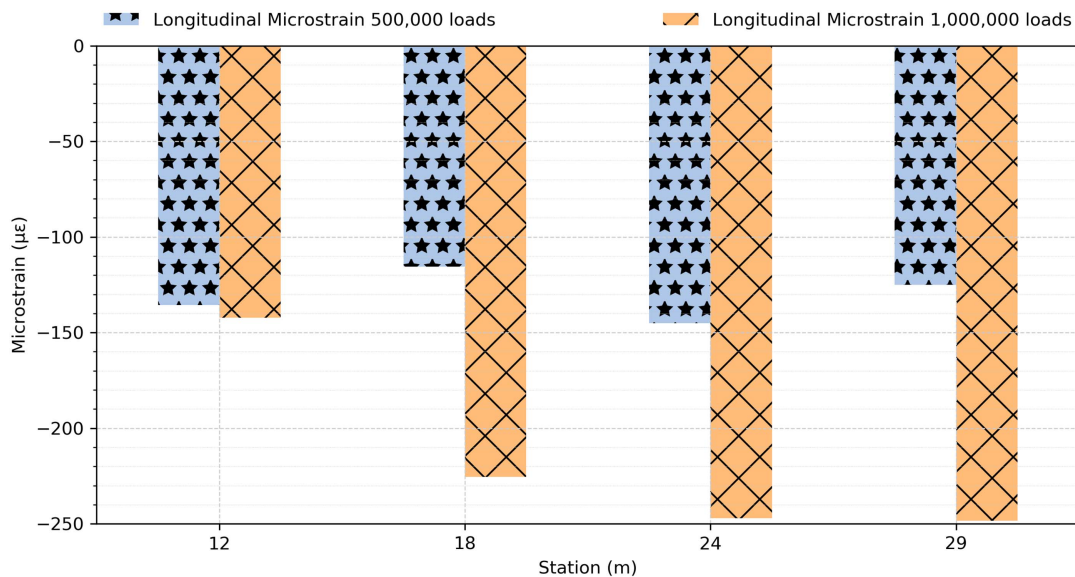


Fig. 19. Longitudinal strain for different stations at 0.5 and 1.0 million load repetitions.

step will focus on implementing a larger number of piezoelectric sensors in an actual in-service road.

Further research should investigate the optimization of the number and location/layout of sensors within the pavement section under real traffic loading conditions.

### Data Availability Statement

Some or all data, models, or code generated or used for this paper are available from the corresponding author by request (raw signals from APT experiment, FWD data, MATLAB code, and temperature profiles).

### Acknowledgments

This work was supported in part by the National Science Foundation (Award CNS 1645783). This paper was carried out as part of

the H2020-MSCA-ETN-2016 receiving funding from the European Union's H2020 Programme for research, technological development and demonstration under Grant Agreement No. 721493.

### References

- Alavi, A. H., H. Hasni, N. Lajnef, and K. Chatti. 2016. "Continuous health monitoring of pavement systems using smart sensing technology." *Constr. Build. Mater.* 114 (Jul): 719–736. <https://doi.org/10.1016/j.conbuildmat.2016.03.128>.
- Aono, K. 2017. "Self-powered sensors to facilitate infrastructural internet-of-things for smart structures self-powered sensors to facilitate infrastructural internet-of-things for smart structures." In *Proc., 13th Int. Workshop on Advanced Smart Materials and Smart Structures Technology*, 1–8. Tokyo, Japan: Univ. of Tokyo. <https://par.nsf.gov/servlets/purl/10069449>.
- Aono, K., H. Hasni, O. Pochettino, N. Lajnef, and S. Chakrabarty. 2019. "Quasi-self-powered Piezo-floating-gate sensing technology for



- continuous monitoring of large-scale bridges." *Front. Built Environ.* 5 (Mar): 29. <https://doi.org/10.3389/fbuilt.2019.00029>.
- Aono, K., and O. Pochettino. 2018. "Quasi-self-powered infrastructurel internet of things: The Mackinac bridge case study." In *Proc., 2018 on Great Lakes Symp. on VLSI, GLSVLSI '18*, 335–340. New York: Association for Computing Machinery. <https://doi.org/10.1145/3194554.3194622>.
- Bahrani, N., J. Blanc, P. Hornych, and F. Menant. 2020. "Alternate method of pavement assessment using geophones and accelerometers for measuring the pavement response." *Infrastructures* 5 (3): 25. <https://doi.org/10.3390/infrastructures5030025>.
- Brown, S. F. 1998. "Developments in pavement structural design and maintenance." *Proc. Inst. Civ. Eng. Transp.* 129 (Nov): 201–206. <https://doi.org/10.1680/itrans.1998.31191>.
- Brown, S. F., and K. R. Peattie. 1974. "The structural design of bituminous pavements for heavy traffic." *Proc. Inst. Civ. Eng.* 57 (1): 83–97.
- Brownjohn, J. M. W. 2007. "Structural health monitoring of civil infrastructure." *Philos. Trans. R. Soc. London, Ser. A* 365 (1851): 589–622. <https://doi.org/10.1098/rsta.2006.1925>.
- Chatti, K., A. H. Alavi, H. Hasni, N. Lajnef, and F. Faridazar. 2016. "Damage detection in pavement structures using self-powered sensors." In Vol. 13 of *Proc., 8th RILEM Int. Conf. on Mechanisms of Cracking and Debonding in Pavements*, edited by A. Chabot, W. Buttlar, E. Dave, C. Petit, and G. Tebaldi. Dordrecht, Netherlands: Springer. <https://doi.org/10.1007/978-94-024-0867-6>.
- Corté, J.-F., and M.-T. Goux. 1996. "Design of pavement structures: The French technical guide." *Transp. Res. Rec.* 1539 (1): 116–124. <https://doi.org/10.1177/0361198196153900116>.
- Del Grosso, A. E. 2013. "Structural health monitoring 2013, a road map to intelligent structures." In *Proc., 9th Int. Workshop on Structural Health Monitoring*, edited by F.-K. Chang. Stanford, CA: Stanford Univ.
- Dessouky, S. H., I. L. Al-Qadi, and P. J. Yoo. 2014. "Full-depth flexible pavement responses to different truck tyre geometry configurations." *Int. J. Pavement Eng.* 15 (6): 512–520. <https://doi.org/10.1080/10298436.2013.775443>.
- Di Graziano, A., V. Marchetta, and S. Cafiso. 2020. "Structural health monitoring of asphalt pavements using smart sensor networks: A comprehensive review." *J. Traffic Transp. Eng.* 7 (5): 639–651. <https://doi.org/10.1016/j.jtte.2020.08.001>.
- DMRB (Design Manual for Roads and Bridges). 2020. *Data for pavement assessment*. CS 229. Republic of Ireland: DMRB.
- Doebbling, S. W., C. R. Farrar, M. B. Prime, and D. W. Shevitz. 1996. *Damage identification and health monitoring of structural and mechanical systems from changes in their vibration characteristics: A literature review*. LA-13070-MS UC-900. New Mexico: Los Alamos National Laboratory.
- EN (European Standards). 2012. *Tests for geometrical properties of aggregates—Part 3: Determination of particle shape—Flakiness index*. EN 933-3:2012. Pilsen, Czech Republic: EN.
- EN (European Standards). 2020a. *Tests for mechanical and physical properties of aggregates—Part 2: Methods for the determination of resistance to fragmentation*. EN 1097-2:2020. Pilsen, Czech Republic: EN.
- EN (European Standards). 2020b. *Tests for mechanical and physical properties of aggregates—Part 8: Determination of the polished stone value*. EN 1097-8:2020. Pilsen, Czech Republic: EN.
- Farrar, C. R., and K. Worden. 2007. "An introduction to structural health monitoring." *Philos. Trans. R. Soc. London, Ser. A* 365 (1851): 303–315. <https://doi.org/10.1098/rsta.2006.1928>.
- Hasni, H., A. H. Alavi, K. Chatti, and N. Lajnef. 2017. "A self-powered surface sensing approach for detection of bottom-up cracking in asphalt concrete pavements: Theoretical/numerical modeling." *Constr. Build. Mater.* 144 (Jul): 728–746. <https://doi.org/10.1016/j.conbuildmat.2017.03.197>.
- Hasni, H., P. Jiao, A. H. Alavi, N. Lajnef, and S. F. Masri. 2018. "Structural health monitoring of steel frames using a network of self-powered strain and acceleration sensors: A numerical study." *Autom. Constr.* 85 (Sep): 344–357. <https://doi.org/10.1016/j.autcon.2017.10.022>.
- Iodice, M., J. M. Muggleton, and E. Rustighi. 2021. "The in-situ evaluation of surface-breaking cracks in asphalt using a wave decomposition method." *Nondestructive Test. Eval.* 36 (4): 388–410. <https://doi.org/10.1080/10589759.2020.1764553>.
- Lajnef, N., K. Chatti, S. Chakraborty, M. Rhimi, and P. Sarkar. 2013. "Smart pavement monitoring system." Accessed December 10, 2017. <http://trid.trb.org/view.aspx?id=1251704>.
- Lajnef, N., M. Rhimi, K. Chatti, L. Mhamdi, and F. Faridazar. 2011. "Toward an integrated smart sensing system and data interpretation techniques for pavement fatigue monitoring." *Comput.-Aided Civ. Infrastruct. Eng.* 26 (7): 513–523. <https://doi.org/10.1111/j.1467-8667.2010.00712.x>.
- Leiva-Villacorta, F., A. Vargas-Nordbeck, J. P. Aguiar-Moya, and L. Loría-Salazar. 2016. "Development and calibration of permanent deformation models." In *The roles of accelerated pavement testing in pavement sustainability: Engineering, environment, and economics*, 573–587. Cham, Switzerland: Springer. [https://doi.org/10.1007/978-3-319-42797-3\\_37](https://doi.org/10.1007/978-3-319-42797-3_37).
- Manosalvas-Paredes, M., A. Navarro Comes, M. Francesconi, S. Khosravifar, and P. Ullidtz. 2017. "Fast falling weight deflectometer (FastFWD) for accelerated pavement testing (APT)." In *Proc., 10th Int. Conf. on the Bearing Capacity of Roads, Railways and Airfields (BCRRA 2017)*, 2235–2241. Boca Raton, FL: CRC Press. <https://doi.org/10.1201/9781315100333-318>.
- Manosalvas-Paredes, M., R. Roberts, M. Barriera, and K. Mantalovas. 2019. "Towards more sustainable pavement management practices using embedded sensor technologies." *Infrastructures* 5 (1): 4. <https://doi.org/10.3390/infrastructures5010004>.
- Marecos, V., S. Fontul, M. de Lurdes Antunes, and M. Solla. 2017. "Evaluation of a highway pavement using non-destructive tests: Falling weight deflectometer and ground penetrating radar." *Constr. Build. Mater.* 154 (Nov): 1164–1172. <https://doi.org/10.1016/j.conbuildmat.2017.07.034>.
- NAPA (National Asphalt Pavement Association) and EAPA (European Asphalt Pavement Association). 2011. *The asphalt paving industry a global perspective*. 2nd ed. Brussels, Belgium: EAPA.
- NEN (Royal Netherlands Standardization Institute). 2020. *Tests for geometrical properties of aggregates—Part 5: Determination of percentage of crushed particles in coarse and all-in natural aggregates*. NEN-EN 933-5. Delft, Netherlands: NEN.
- Nguyen, M. L., J. Blanc, J. P. Kerzrého, and P. Hornych. 2013. "Review of glass fibre grid use for pavement reinforcement and APT experiments at IFSTTAR." *Road Mater. Pavement Des.* 14 (May): 37–41.
- Robbins, M. M., C. Rodezno, N. Tran, and D. Timm. 2017. *Pavement ME design—A summary of local calibration efforts for flexible pavements*. NCAT Rep. No. 17-07. Auburn, AL: National Center for Asphalt Technology.
- Sohn, H., C. R. Farrar, F. M. Hemez, and J. J. Czarnecki. 2003. *A review of structural health monitoring literature 1996–2001*. Santa Fe, NM: Los Alamos National Laboratory.
- Susanna, A., M. Crispino, F. Giustozzi, and E. Toraldo. 2017. "Deterioration trends of asphalt pavement friction and roughness from medium-term surveys on major Italian roads." *Int. J. Pavement Res. Technol.* 10 (5): 421–433. <https://doi.org/10.1016/j.ijprt.2017.07.002>.
- Ullidtz, P., and H. J. Ertman Larsen. 1989. "State-of-the-art stress, strain and deflection measurements." In *Proc., Symp. on the State-of-the-Art of Pavement Response Monitoring Systems for Roads and Airfields*, 148–161. Hanover, NH: Army Cold Regions Research and Engineering Laboratory.
- Verma, S. K., S. S. Bhaduria, and S. Akhtar. 2013. "Review of nondestructive testing methods for condition monitoring of concrete structures." *J. Constr. Eng.* 2013 (2008): 1–11. <https://doi.org/10.1155/2013/834572>.
- Xue, W., D. Wang, and L. Wang. 2012. "A review and perspective about pavement monitoring." *Int. J. Pavement Res. Technol.* 5 (5): 295–302. [https://doi.org/10.6135/IJPRT.ORG.TW/2012.5\(5\).295](https://doi.org/10.6135/IJPRT.ORG.TW/2012.5(5).295).
- Xue, W., L. Wang, D. Wang, and C. Druta. 2014. "Pavement health monitoring system based on an embedded sensing network." *J. Mater. Civ. Eng.* 26 (10): 04014072. [https://doi.org/10.1061/\(ASCE\)MT.1943-5533.0000976](https://doi.org/10.1061/(ASCE)MT.1943-5533.0000976).